

ANALYSIS OF STRESS OF THE EPDM RUBBER APPLIED IN AUTOMOTIVE SEALS USING FEA

Rafael Hajime Tosi Ueda, hajimeueda@yahoo.com.br

Federal University of São João del Rei – UFSJ, Praça Frei Orlando, 170 – Centro, CEP 36.307-352, São João Del Rei-MG

Carlos Henrique Lauro, caiquelauro@gmail.com

Federal University of São João del Rei – UFSJ, Praça Frei Orlando, 170 – Centro, CEP 36.307-352, São João Del Rei-MG

Lincoln Cardoso Brandão, lincoln@ufsj.edu.br

Federal University of São João del Rei – UFSJ, Praça Frei Orlando, 170 – Centro, CEP 36.307-352, São João Del Rei-MG

Abstract. *Seals have wide application in automotive products. It is responsible for the car sealing in several parts such as doors, the air intake seal cowl, outer waist belt, and air intake seal light, etc. The study of strain and stress is very important in order to understand the behavior of polymeric materials, which are generally submitted to great workload variation and environmental influence. This study of EPDM rubber was carried out to define the strain, stress and yield stress. Tensile and compression tests were carried on workpieces with 100 mm of length. The data was acquired using the Qmat software. A Finite Element Analysis using the MSC Marc Mentat™ was conducted and compared with experimental tests. The results showed an increase of efforts proportional to bulb thickness. A proportional increase of compression efforts for different displacements was significant. Moreover, physical parameters such as length, thickness, and friction coefficient changed the strain rate and stress.*

Keywords: *Door Seals, EPDM Rubber, Finite Element Analysis, Stress.*

1. INTRODUCTION

Rubber products have a wide application in the automotive industries. The application of the rubber products in the automotive industry can be divided into tires that are consumable products having a short life span and seals that last longer. Generally, seals are manufactured to last as long as the automobiles. Thus, recycling of these products is more appropriate for tires due to their shorter time of use. According Fukumori et al. (2002), recycling of waste materials is of growing importance for all the industries in the world. For rubber products, the automotive and transportation industries are the biggest consumers of new rubber.

The main applications of the rubber seals in automobiles are: door seals, secondary door seals, air intake seal cowls, air intake seal lights, liftgate seals, ditch molding and outer waistbelts. These are in turn divided into dynamic and static seals. The main purpose of the door seals e.g. is to provide a perfect seal between the door and the automobile against extreme climatic conditions, to reduce external noise, to contribute to the quality of opening and closing of the door, and to protect the passengers against the aggressive environment (Copper Standard Automotive, 2009).

Among various polymeric materials, EPDM has been of great interest to engineers particularly in the automotive sector. Rubber EPDM is the main raw material of the seals and belongs to the group of the thermo polymers to which a third monomer – Diene – is added in order to introduce unsaturation to the chain. According Bouchart et al. (2008) the use of EPDM-PP blends has been continuously growing in various industrial domains since several decades. As it is possible to mix Ethylene Propylene Diene Monomer (EPDM) and polypropylene (PP) in any ratio, there is theoretically a wide spectrum of materials from elasticized PP to EPDM rubber reinforced with thermoplastics.

Many studies have been conducted about the mechanical behavior of PP/rubber blends (Zebarjad et al. 2004). Four main approaches have been proposed in these studies. The first approach concerns the influence of interfacial adhesion and its role on compatibility between the matrix and the elastomeric phase (Baia et al., 2004). The second group concentrates on the effects of elastomer content, particle size, and particle distribution on the mechanical behavior (Zebarjad et al., 2004). In fact, deformation behavior during tensile loading is still a matter of controversy among researchers. For example, Jange et al. (1985) reported that the mechanism of deformation in PP/EPDM blend is crazing. Also Jang et al. (1985), Karger–Kocsis and Csikai (1987) showed that there is a relationship between crazing and crystalline morphology of the blend.

The project of a dynamic seal can present a system of a simple bulb or a system of two bulbs. The system of two bulbs generally is used when there are great gaps between the doors and chassis of the automobile. Another component in the dynamic seals and the static seals is the lip. It has the function to give better appearance to the seal, as well as to fix it to the flange of the vehicle. Generally, these lips are of thermoplastic dense or EPDM rubber. Thermoplastic material already is used in the design of the dynamic seal. It is used more in the seals of windshields and windows. Some studies have shown that the use of thermoplastic materials in the design of the seals reduces by 30% the weight of the product (Bedard, 2008).

This paper presents the validation of the seals using software MSC Marc Mentat™ based on the theoretical models for hyperelastic materials that describe the behavior of the material through the strain energy. These models are used

generally to describe the nonlinear behavior of the elastomeric materials and are valid when the theory of great strain is used. In problems involving great deformations, geometric non-linearity must also be taken into account.

2. METHODOLOGY

The validation of the seals through software MSC Marc Mentat™ used models for hyperelastic materials describing the behavior of the material through the strain energy. This method was used to describe the nonlinear behavior of the elastomeric materials being validated using the theory of great strain. In the experiments the material initially was considered isotropic. However, when the material was submitted to a tensile force in the orientation of the molecules movement, anisotropy must be considered. With this in mind, the generation of that anisotropy is assumed in the direction of the strain effort. For this reason, the material can be considered isotropic and the potential energy of strain was formulated as a function of the invariants of strain, as the Eq. (1), (2) and (3).

$$I_1 = \lambda_1^2 + \lambda_2^2 + \lambda_3^2 \quad (1)$$

$$I_2 = \lambda_1^2 \cdot \lambda_2^2 + \lambda_2^2 \cdot \lambda_3^2 + \lambda_3^2 \cdot \lambda_1^2 \quad (2)$$

$$I_3 = \lambda_1^2 \cdot \lambda_2^2 \cdot \lambda_3^2 \quad (3)$$

Where λ_1, λ_2 e λ_3 are the mean extensions defined by Eq. (4):

$$\lambda_i = \frac{(L_i + u_i)}{L_i} \quad (4)$$

The model of Mooney-Rivlin was applied for the calculations on EPDM rubber considering it as incompressible according Eq. (5). Another mathematical model had used the Foam model, simulating the behavior of rubber EPDM of the sponge type, considering the compressibility of the material.

$$\lambda_1 \cdot \lambda_2 \cdot \lambda_3 = 1 \quad (5)$$

2.1. Mooney-Rivlin model

The potential energy was calculated according with the Mooney-Rivlin model presented in Eq. (6).

$$U = C_1(\bar{I}_1 - 3) + C_2(\bar{I}_2 - 3) + \frac{1}{D_1}(J^{el} - 1)^2 \quad (6)$$

Where C_1, C_2 and D_1 are parameters of the material, \bar{I}_1 and \bar{I}_2 are the invariants of strain. For the situations where the nominal strain is small or significantly great (<100%), this model is sufficiently useful. The D_1 constant is related to the degree of incompressibility of the material, therefore when it is zero the material is considered incompressible. Preliminary tests had shown that for deformation 30% of (or 30% less than?) the maximum deformation of the specimen the curve stress-strain is almost linear. In order to simplify the characterization of the material, it was decided then to parametrizar only the C_1 constant of the material. Thus, the potential strain energy was given by Eq. (7).

$$U = C_1(\bar{I}_1 - 3) + \frac{1}{D_1}(J^{el} - 1)^2 \quad (7)$$

This model is also known as Neo-Hookeano model. The Mooney-Rivlin is the model more used to characterize the hyperelastic materials, because the modification of the C_1 parameter allows this characterization.

2.2. Foam model

The model of the potential energy using the Foam model can be written according Eq. (8).

$$U = \sum_{n=1}^N \frac{\mu_n}{\alpha_n} [\lambda_1^{\alpha_n} + \lambda_2^{\alpha_n} + \lambda_3^{\alpha_n} - 3] + \sum_{n=1}^N \frac{\mu_n}{\beta_n} (1 - J^{\beta_n}) \quad (8)$$

Where λ_i is the main extension and μ_i , α_i and β_i are the constants related to the properties of the material.

2.3. Mechanical and simulation Seals tests

The experiments of validation of the dynamic and static seals were based on the method of the correlation between the mechanical tests and the Finite Element Analysis using the software MSC Marc Mentat™. The tests of compression had been carried out using a dynamometer with a compression speed of 10 mm.min⁻¹ with specimens of 100 mm in length, and the acquisition data was obtained using Qmat software™, as shown in Fig. (1). The objective of this test is to define the force acting on seals in function of the distance between the up and bottom tray of the dynamometer. The compression test was conducted on a linear table that avoided the radial forces due to the friction between the tray and the seals, thus obtaining the results of the efforts through just one vector component.

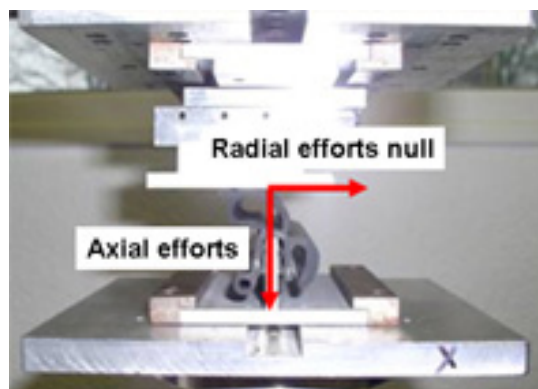


Figure 1 - Linear table used in the tests of plain compression.

The compression tests had the objective of simulating the closing of a door. When an elastomer is tested in a cyclical situation, a reduction of the load is necessary to get the same elongation, and this phenomenon is called Mullins effect. After certain time without compression the material returns to its initial form. Figure 2 shows the three liftgate seals tested.




Profile name	P12 – mastic	Metzeler	P12 – Cordon Norton
Section format of the liftgate seals tested			

Figure 2 - Detail of the three liftgate sections tested

The geometric of the variable as thickness and diameter of the bulb are the parameters that have influence on the evolution of the forces of compression as well as the choice of rubber EPDM type sponge. Table (2) shows the influence of the thickness of the bulb on the increase of the forces of compression, according Bedard (2008). Due to the difficulty of obtaining a constant section of the bulb in the extrusion process of the EPDM rubber seals of the sponge type, it is common to not get accurate results equal to predicted by the calculation. Thus, the results of the calculations and the tests must be conducted with the objective of evaluating the influence of geometry and how much this varies in the process. The inner blue-green line of Fig. 3 shows a variation of 0.2 mm in the thickness of the bulb.

Table 1 – Efforts of strain for different sections

Inner variation	Effort (N.dm ⁻¹)	% Maximum Strain
Standard section (.dxf)	3.475	22
Section + 0.123 mm	4.545	23
Section + 0.190 mm	5.196	25
Section + 0.247 mm	5.745	25

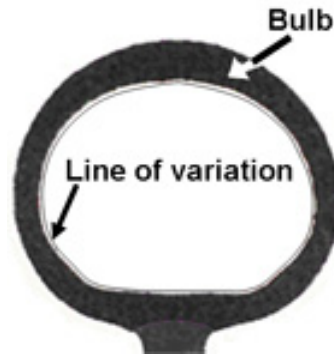


Figure 3 - Example of the bulb variation thickness

The test had been carried out at 23°C and 50% HR on three specimens of each profile to assure the accuracy of the results.

3. ANALYSIS OF RESULTS

3.1. Experimental tests

Figure (4) shows the result of the compression tests carried out at 23°C and 50% HR with specimens of each one of the three liftgate seals, as shown in Fig.(2). The profile chosen was the Metzeler due to a range of displacement between 10 and 22 mm and the lesser deformation force. Thus, the Metzler profile was chosen for the experimental tests and the simulations of the new bulb. Figure (5) shows the compression tests carried out with the Metzeler profile with a variation of ±10%. of displacement.

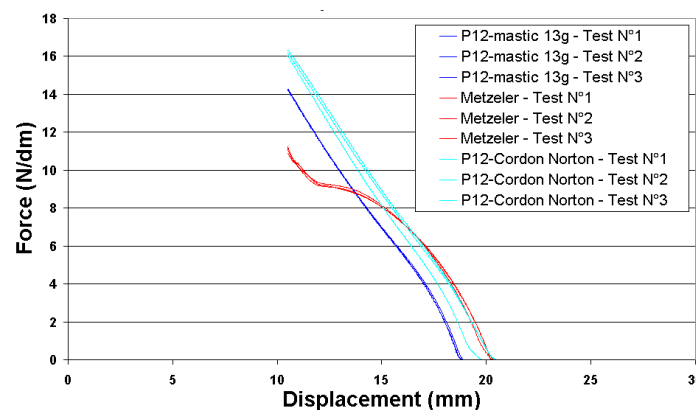


Figure 4 – Displacement curves for the three liftgate seals tested.

Once the ideal profile was defined, three curves of compression forces were then plotted considering a variation of ±10% of these values, so that any simulated force inside this interval was considered acceptable. Afterwards, tests of insertion and extraction were carried out with specimens of 100 mm in length. These tests had the aim to simulate the assembly and the disassembly of the seals on the specific flanges of the automobiles. The speed of insertion and extraction used in the tests was 100 mm.min⁻¹. The geometric variables such as thickness of the lip and length and angle

of inclination were the parameters of influence during this test. Errors generated during the extrusion process such as, for example, the increase in the thickness of the lip, tend to cause excessive lip rigidity. The tests of insertion and extraction were carried out with the same three liftgate seals of Fig. (2), each experiment being replicated 3 times with flanges with thicknesses of 1.2 and 1.6 mm. Figure (6) shows a test of insertion for a flange of 1.6 mm.

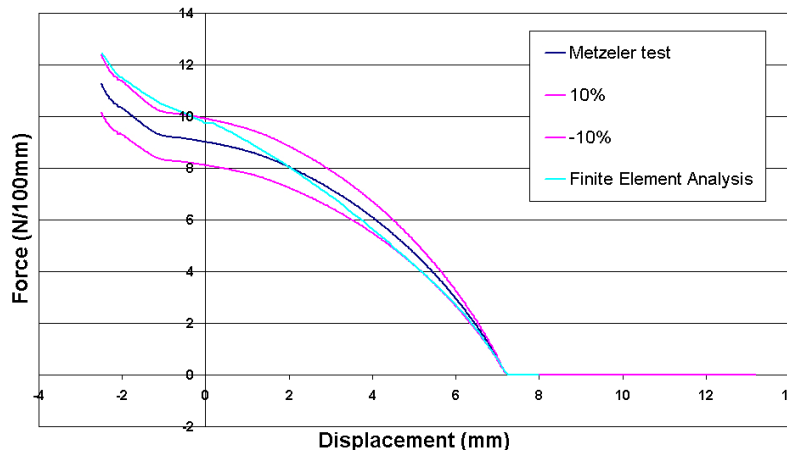


Figure 5 – Comparison between displacement curves for the Metzeler bulb with $\pm 10\%$ and FEA.

The profile chosen for the design of a new clamp was the P12 mastic, so that the forces of insertion and extraction corresponded to the standard values of the automotive industries. This way, the arithmetic mean of the values of the insertion and extraction efforts was obtained, and the curves were plotted with a tolerance of $\pm 10\%$, where the values of maximum insertion and minimum extraction must be within this range.

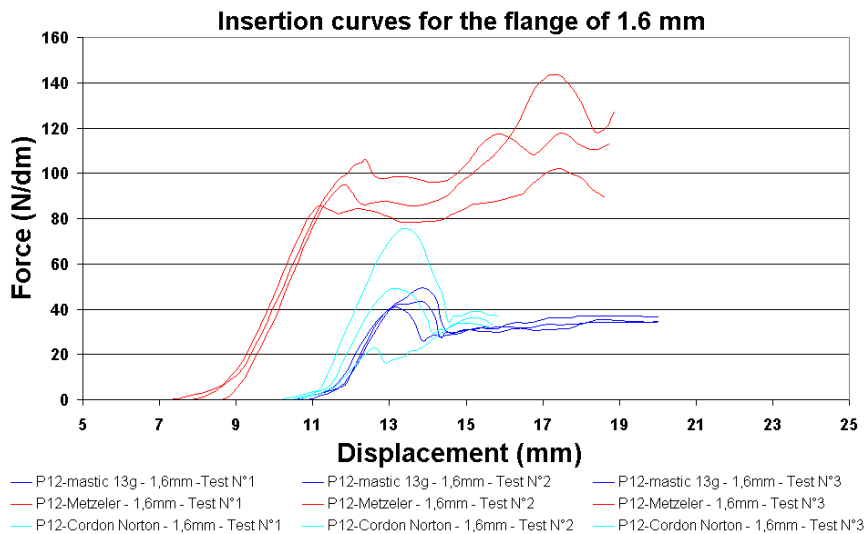


Figure 6 – Test of insertion in the flange of 1.6 mm for the three liftgate seals.

3.2. Simulation with MSC Marc Mentat™

The simulations of the insertion and extraction tests using the method of finite elements had been two dimensional, allowing analyzing the behavior of the seals before and after the extrusion. The objective of this test was to define the thrust force of compression, insertion, extraction and strain. In order to simulate the characteristics of the real profile seals, it was necessary digitalize the extrusion profile of the seals and construct the contour using the software Solid Edge™. Afterwards, it was possible to be carried through the profile exported for the simulation software creating files in the format “dxP” or “dwg”. The creation of the mesh had as objective to distinguish the different materials of the seals and to refine the elements resulting in more accurate data. The generated elements had been quadrature, but also the formation of triangle elements was necessary. For the creation of the theoretical model, the curves of the profile had been subdivided in spacing of 0.2mm. Table 2 shows the data of the two models with the number of nodes and quadratic and triangle elements.

Table 4 – Data of the simulation model

Number of elements	Metzeler profile	P12 Mastic Profile
Triangles	0	0
Quadrates	9,281	9,905
Number of nodes	10,064	10,677

The bulbs initially had been inserted in a resin for the measurement of the details of the profile. Therefore, the digitalization of the profile using software Solid Edge™ was made. Since the profile was redesigned the exportation of each profile points to software of FEA was possible and the simulation could be started. Figure 7 shows the construction of the mesh after the digitalization and with the profiles defined by software MSC Marc Mentat™.

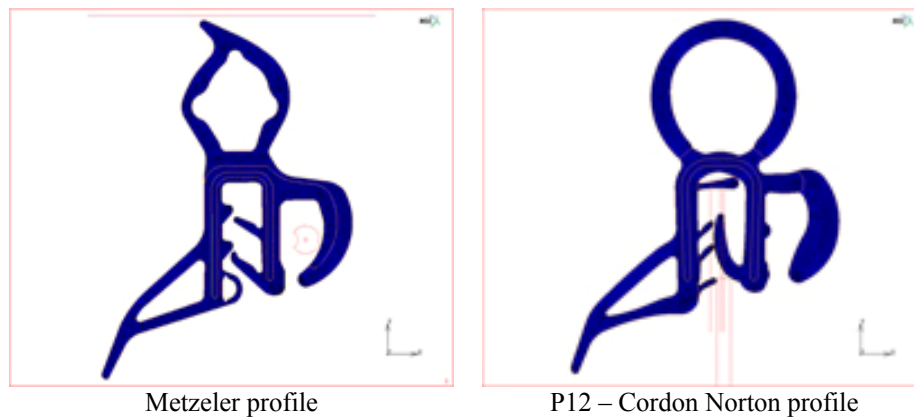


Figure 7 – Profiles defined in the MSC Marc Mentat™ software.

Dense rubber EPDM was simulated by the model of “Mooney-Rivlin” with coefficient established according to Bouchart et al., (2008). Rubber EPDM type sponge uses the formularization like “Foam” with the objective to represent the compressibility of the bulb and parts where they are applied.

Table 5 –Constants of the model

Material	C1	μ	α	β
P127G204	0.95	-	-	-
P225T201S_foam	-	0.185	10	-0.5
P225M421_foam	-	0.090	10	-0.5
P226H200	0.25	-	-	-

In the experimental tests a dimensional variation of $\pm 2.5\text{mm}$ was applied above and below the standard position. The calculation of the compression forces was given in these three positions, according as shown in Fig. (8). The results of the maximum or stresses for experimental data and Finite Element Analysis are represented in the Table. (6). The graphs show a good relation between the experimental and simulated results where it can be observed that the increase of the compression force occurs in a range of $\pm 10\%$ of tolerance. Therefore the result shows that the FEA value was within the standards defined for the automobile industry.

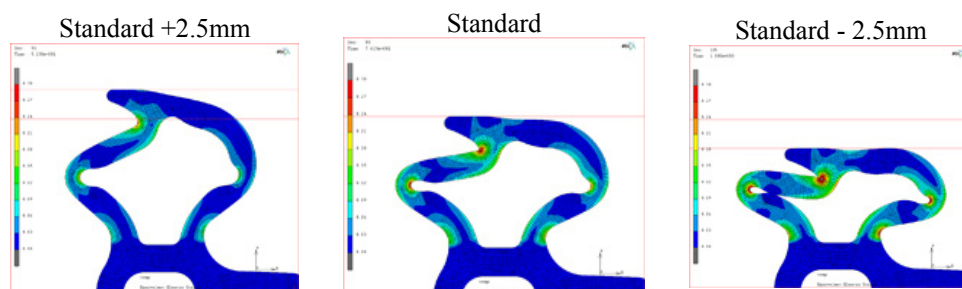


Figure 8 – Standard Compression and variation of $\pm 2.5\text{mm}$ for the Metzeler profile.

Table 6 – Values of the compress efforts

Test	Force (N/100mm)		
	Standard +2.5mm	Standard	Standard -2.5mm
Test with -10%	6.9	8.1	10.1
Standard test	7.6	9.0	11.3
Test with +10%	8.4	9.9	12.4
Finite Element Analysis	7.5	9.7	12.4

The maximum value of insertion does not exceed 80 N.dm^{-1} for the flange of 1.6 mm, and the extraction is not less than 100 N.dm^{-1} for the flange of 1.2mm, according Copper Standard Automotive (2009). Figures (9a) and (9b) illustrate the simulation of insertion of the flange of 1.6 mm and extraction of the flange of 1.2 mm, respectively.

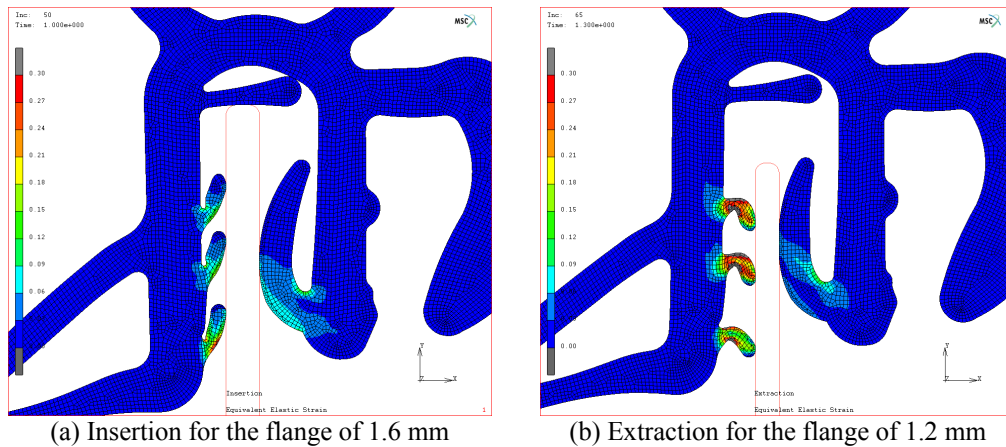


Figure 9 – Details of the insertion in the flange of 1.6 mm and extraction in the flange of 1.2mm for Metzeler profile.

Table (7) shows the values of insertion, extraction and Finite Element Analysis of the profile tested. It can be observed that the extraction force is three times superior to the insertion force. The objective is to have the easiest possible assembly of the seals in the industry, but resulting in a more difficult disassembly when the component is required by the job. The results of the FEA values are shown alongside the experimental tests, demonstrating the efficiency of the validation of the experimental tests of insertion and extraction of the seals. Figure 10 shows the experimental standards with the variation of $\pm 10\%$ of tolerance for the test of insertion of the P12 mastic seals. Therefore, it can be observed that the results of the FEA were similar to the experimental tests. The maximum values of insertion were less than the experimental values, but comparing them with the data of the Table (7) it can be seen that the values of the simulation were inside of the same range of the experimental values with maximum error of variation of 6%.

Table 7 – Results of the insertion and extraction forces.

Test	Force (N/100 mm)	
	Insertion	Extraction
Test with -10%	35.6	98.5
Standard test	39.6	109.4
Test with +10%	43.6	120.4
Finite Element Analysis	35.7	113.8

As a result, it was possible with the simulation to do the optimization of the profile using only the data obtained for the simulation technique. However, the optimization of the profile was only carried out in the lower part of the seals where the lips have the objective to simultaneously better fix the part preventing the extraction and minimize the insertion forces during the assembly on the flange. Figure (11a) shows the format of the standard geometry. Generally the profile is formed by two different materials, aluminum and the P128d236 rubber, and for this reason the technical characteristics of each material had been considered during the simulation.

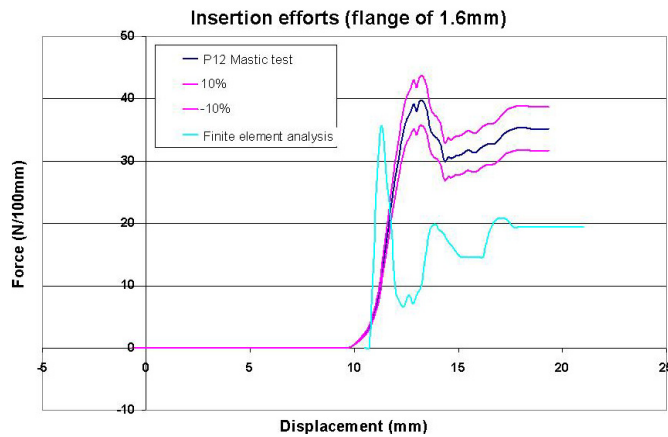


Figure 10 – Details of the experimental insertion forces and FEA for the flange of 1.6 mm.

After all the stages of simulation using the technique of FEA with the creation of the mesh, the definition of the materials was verified with the strain of the profile and the maximum force of insertion. Thus, due to the contact between the two lips, one high force of insertion was observed in the standard model, according to Fig. (11b). The strategy used was the optimization of the section with the reduction of the length of the first lip, thus minimizing the contact with the upper lip as is shown in Fig. (11c).

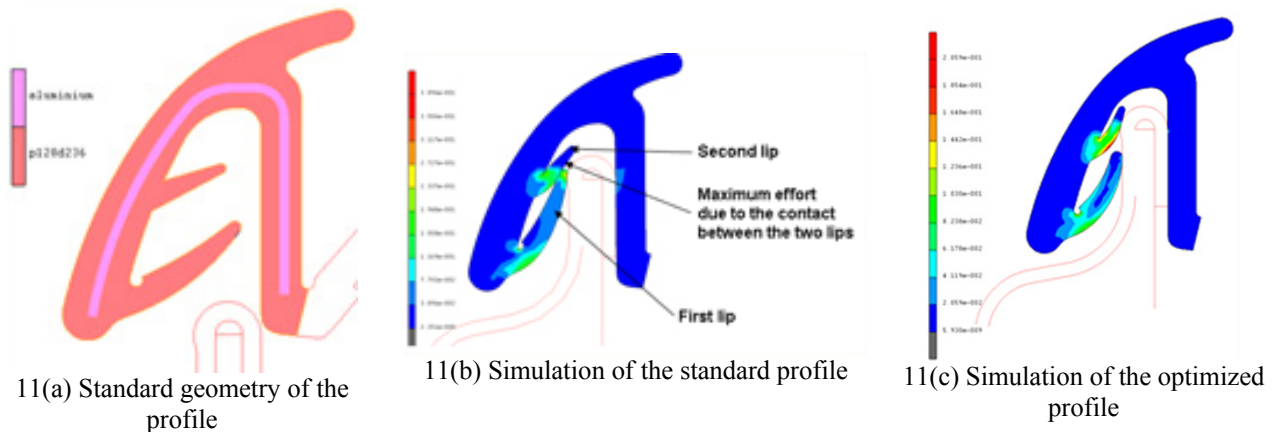


Figure 11 – Details of the optimization the Mezteler profile using FEA.

This way, a graph with the forces of insertion versus the distance of displacement on the assembly flange of the seals can be plotted. Figure (12) shows the result of the force for the displacement on the flange, where it was observed that the initial efforts with the model of standard geometry had been 4 times more that the values obtained for the optimized model. Table 8 shows the maximum results of insertion for the initial profile and the optimized profile. Therefore, it can be considered that the FEA effectively defined the optimum profile of the seals, without which this component lost its efficiency as defined in the project.

Table 8 – Maximum values of insertion

Maximum value of insertion [N/dm]	Initial Section	Optimized section
		163.5

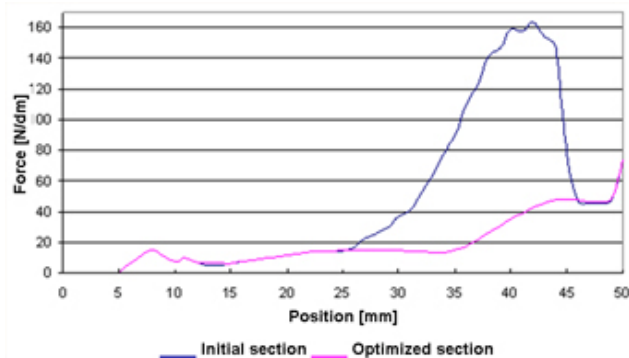


Figure 13 – Graph of the insertion Force x distance of displacement on the flange

4. CONCLUSIONS

In accordance with the results, the following conclusions can be reached:

- ✓ A proportional increase of the compression forces in function of the displacement of the tray for the different set ups can be observed. The physical parameters such as thickness and diameter of the bulb, and the choice of the friction coefficient between the tray and the specimen, changed the results significantly;
- ✓ The studies showed an increase of 65% in the compression forces proportional to an increase of 0.247 mm for the thickness of the bulb;
- ✓ The Finite Element Analysis of the compression forces showed a good correlation with the experimental tests during the displacement of the tray;
- ✓ Physical parameters as length, thickness and inclination of the lips, as well as the friction coefficient used modified the variation of the strain in maximum stress (?);
- ✓ The biggest force of insertion occurs when the flange has contact with the two first lips of the seals. Afterwards, a reduction of the stress with a gradual increase is observed during the contact with the others two lips;
- ✓ The biggest force of extraction occurs during the inversion of the positioning of the lower lips of the seals. This is normal behavior when it is necessary to get higher values of extraction;
- ✓ The graphs of the insertion efforts and extraction almost always are different from the obtained real forces. However, it can be observed that the maximum and minimum values of insertion and extraction are within the tolerances standards.

5. ACKNOWLEDGEMENTS

The authors would like to thank the Copper Standard Automotive for the permitting the development of the project in the company in Vitré, France.

6. REFERENCES

- Baia, Shu-Lin, , G'Sellb, C. ; Hiverc, J.M.; Mathieuc, C. 2004 "Microstructures and mechanical properties of polypropylene/polyamide 6/polyethelene-octene elastomer blends". *Polymer*, v.45 (90), pp. 3063-3071
- Bedard, L., 2008 "Caractérisation dynamique des joints automobiles". 49p. Dissertação (Graduação em Engenharia Mecânica) - Université du Québec à Trois-Rivières, Trois-Rivières, QC G8Z, Canada, 2008.
- Bouchart, V.; Bhatnagar, N; Brieu, M.; Ghosh, A.K.; Kondo, D., 2008 "Study of EPDM/PP polymeric blends: mechanical behavior and effects of compatibilization" *Comptes Rendus Mecanique*, v. 336, pp. 714–721.
- Copper Standard Automotive, 2009 "Body and Chassis – products and innovations", http://www.cooperstandard.com/body_chassis.php, acesso em 04/04/2009.
- Fukumori, K. et al., 2002, "Recycling technology of tire rubber", *JSAE Review*, v. 23, pp. 259–264.
- Jange, B.Z.; Ulmann, D.R.; Vander Sande, J.B., 1985 "Crazing in Polypropylene" *Journal Applied Polymer Science*, v.30, pp. 24-85.
- Karger-Kocsis, J.; Friedrich, K., 1987 "Microstructural details and the effect of testing conditions on the fracture toughness of injection-moulded poly(phenylene-sulphide) composites", v.22, n.3, pp. 947-961.
- Zebarjad, S. M.; Bagheri, R.; Lazzeri, A.; Serajzadeh, S., 2004, "Dilatational shear bands in rubber-modified isotactic polypropylene" *Materials & Design*, v. 25(3), pp. 247-250.

7. RESPONSIBILITY NOTICE

The authors are the only responsible for the printed material included in this paper.